

# Wires, Plates, Flowers, Needles, and Core–Shells: Diverse Nanostructures of Gold Using Polyaniline Templates

P. R. Sajanlal, T. S. Sreeprasad, A. Sreekumaran Nair,<sup>†</sup> and T. Pradeep\*

*DST Unit on Nanoscience (DST UNS), Department of Chemistry and Sophisticated Analytical Instrument Facility, Indian Institute of Technology Madras, Chennai-600 036, India*

*Received November 17, 2007. In Final Form: January 16, 2008*

A simple and versatile method for the synthesis of a wide range of polyaniline (PANI)-based 1D and 2D gold nanostructures of uniform size distribution with high colloidal stability is demonstrated. All the nanostructures were synthesized from oligoaniline-coated gold nanoparticle precursors. The nanostructures include nanowires of various sizes, nanoplates, and flower-like nanoparticles. These nanowires showed a pH-dependent shape transformation. Needle-like aggregates of Au/PANI were formed as the pH of the nanowire solution changed to 2.5. At higher pH (10.2), nanowires converted into spherical nanoparticles. Core–shell particles of Au/PANI composites have been achieved by the reversal of the pH of the nanowire from 10.2 to 2.9. The morphology of the nanostructures was studied by TEM and SEM. FTIR, UV–vis, XRD, and LDIMS were utilized for the characterization of the chemical composition of the nanostructures. A mechanism for the nanowire growth is proposed.

## Introduction

Studies of anisotropic metal nanostructures have been attractive to scientists in the past few years due to their extensive applications in catalysis,<sup>1</sup> sensing,<sup>2</sup> optoelectronics,<sup>3</sup> and surface enhanced Raman scattering (SERS).<sup>4</sup> Several such structures have been reported using various synthetic approaches. Diverse nanostructures of gold such as wire,<sup>5</sup> rod,<sup>6</sup> triangle,<sup>7</sup> ribbon,<sup>8</sup> star,<sup>9</sup> multipod,<sup>10</sup> and tadpole<sup>11</sup> have been synthesized in solution. The unusual optical and electrical properties of these metal nanostructures are exploited for fabricating devices. As a result, significant attention has been paid to the shape controlled synthesis of 1D nanostructures. In particular, composites of metal incorporated polymer nanostructures are exciting systems to investigate the possibility of designing functional architectures, because of the diverse chemical and physical properties exhibited by the metal core and the polymeric shell. Among the conducting

polymers, polyaniline (PANI) is a well studied system having large number of applications in nanoelectronics,<sup>12</sup> inkjet printing,<sup>13</sup> opto-microelectronics, photonics,<sup>14</sup> chemical and electrochemical sensors,<sup>15</sup> and biology.<sup>16</sup> Various methods have been reported for the synthesis of one-dimensional nanostructures of PANI such as nanofibres<sup>17</sup> and nanotubes.<sup>18</sup> Metal nanoparticles supported on PANI can also be used as potential candidates for organic catalysis,<sup>19</sup> because PANI can act both as a reducing agent and as a stabilizer. It is known that PANI nanofibers decorated with Au nanoparticles exhibit nonvolatile memory behavior.<sup>20</sup> Moreover, PANI is a technologically important and stable conducting polymer due to its tunable electronic conductivity by both oxidation–reduction and acid–base chemistry.

Recently, various techniques have been developed to achieve coaxial metal–polymer nanostructures.<sup>21</sup> However, very few attempts have been reported to date for the synthesis of anisotropic metal nanostructures using PANI. Huang et al.<sup>22</sup> synthesized gold/PANI (Au/PANI) coaxial nanocables through a self-assembly process in the presence of chloroauric acid (HAuCl<sub>4</sub>) as the oxidant and *d*-camphor-10-sulfonic acid (CSA) as the dopant. Au/PANI composites with a particle size of 26 nm have been synthesized using hydrogen peroxide, which acts both as a reducing agent and as an oxidizing agent.<sup>23</sup> Synthesis of Au/

\* Corresponding author. Email: pradeep@iitm.ac.in. Fax: 91-44-2257-0545/0509.

<sup>†</sup> Present address: Graduate School of Material Science, Department of Material Science, University of Hyogo, 3-2-1 Koto, Kamigori-Cho, Akougun, Hyogo 678-1297, Japan.

(1) (a) Chen, M.; Goodman, W. *Acc. Chem. Res.* **2006**, *39*, 739. (b) Lewis, L. N. *Chem. Rev.* **1993**, *93*, 2693.

(2) Haes, A. J.; Van Duyne, R. P. *J. Am. Chem. Soc.* **2002**, *124*, 10596.

(3) Kamat, P. V. *J. Phys. Chem. B* **2002**, *106*, 7729.

(4) (a) Nie, S.; Emory, S. R. *Science* **1997**, *275*, 1102. (b) Zhang, J.; Li, X.; Sun, X.; Li, Y. *J. Phys. Chem. B* **2005**, *109*, 12544. (c) Campion, A.; Kambhampati, P. *Chem. Soc. Rev.* **1998**, *27*, 241.

(5) (a) Hu, J. T.; Odom, T. W.; Lieber, C. M. *Acc. Chem. Res.* **1999**, *32*, 435. (b) Wiley, B.; Sun, Y.; Mayers, B.; Xia, Y. *Chem.—Eur. J.* **2005**, *11*, 454. (c) Sun, Y.; Xia, Y. *Science* **2002**, *298*, 2176. (d) Pei, L.; Mori, K.; Adachi, M. *Langmuir* **2004**, *20*, 7837. (e) Minelli, C.; Hinderling, C.; Heinzelmann, H.; Pugin, R.; Liley, M. *Langmuir* **2005**, *21*, 7080.

(6) (a) Liao, H.; Hafner, J. H. *Chem. Mater.* **2005**, *17*, 4636. (b) Kim, F.; Song, J. H.; Yang, P. D. *J. Am. Chem. Soc.* **2002**, *124*, 14316. (c) Sreeprasad, T. S.; Samal, A. K.; Pradeep, T. *Langmuir* **2007**, *23*, 9463.

(7) (a) Shankar, S. S.; Rai, A.; Ankamwar, B.; Singh, A.; Ahmad, A.; Sastry, M. *Nat. Mater.* **2004**, *3*, 482. (b) Millstone, J. E.; Park, S.; Shuford, K. L.; Qin, L.; Schatz, G. C.; Mirkin, C. A. *J. Am. Chem. Soc.* **2005**, *127*, 5312. (c) Sajanlal, P. R.; Pradeep, T. *Adv. Mater.* **2008**, *20*, 980.

(8) Swami, A.; Kumar, A.; Selvakannan, P. R.; Mandal, S.; Pasricha, R.; Sastry, M. *Chem. Mater.* **2003**, *15*, 17.

(9) Nehl, C. L.; Liao, H. W.; Hafner, J. H. *Nano Lett.* **2006**, *6*, 683.

(10) Hao, E.; Bailey, R. C.; Schatz, G. C.; Hupp, J. T.; Li, S. *Nano Lett.* **2004**, *4*, 327.

(11) Hu, J.; Zhang, Y.; Liu, B.; Liu, J.; Zhou, H.; Xu, Y.; Jiang, Y.; Yang, Z.; Tian, Z. *J. Am. Chem. Soc.* **2004**, *126*, 9470.

(12) (a) Novak, P.; Mueller, K.; Santhanam, K. S. V.; Has, O. *Chem. Rev.* **1997**, *97*, 207. (b) MacDiarmid, A. G. *Angew. Chem., Int. Ed.* **2001**, *40*, 2581.

(13) Ngamna, O.; Morrin, A.; Killard, A. J.; Moulton, S. E.; Smyth, M. R.; Wallace, G. G. *Langmuir* **2007**, *23*, 8569.

(14) Holdcroft, S. *Adv. Mater.* **2001**, *13*, 1753.

(15) Virji, S.; Huang, J.; Kaner, R. B.; Weiller, B. H. *Nano Lett.* **2004**, *4*, 491.

(16) Liu, J.; Tian, S.; Knoll, W. *Langmuir* **2005**, *21*, 5596.

(17) (a) Huang, J.; Virji, S.; Weiller, B. H.; Kaner, R. B. *J. Am. Chem. Soc.* **2003**, *125*, 314. (b) Huang, J.; Kaner, R. B. *J. Am. Chem. Soc.* **2004**, *126*, 851.

(c) Wei, Z. X.; Zhang, Z. M.; Wan, M. X. *Langmuir* **2002**, *18*, 917. (d) Li, W.; Wang, H. L. *J. Am. Chem. Soc.* **2004**, *126*, 2278.

(18) Huang, J.; Kaner, R. B. *Angew. Chem., Int. Ed.* **2004**, *43*, 5817.

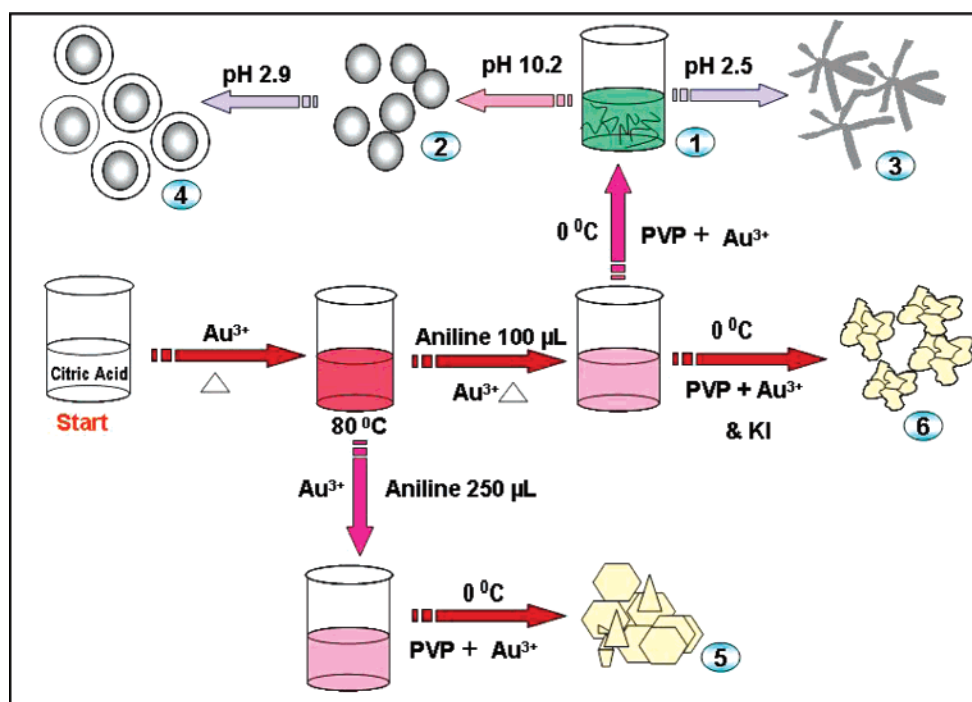
(19) Gallon, B. J.; Kojima, R. W.; Kaner, R. B.; Diaconescu, P. L. *Angew. Chem., Int. Ed.* **2007**, *46*, 1.

(20) Tseng, R. J.; Huang, J. X.; Ouyang, J. Y.; Kaner, R. B.; Yang, Y. *Nano Lett.* **2005**, *5*, 1077.

(21) (a) Lu, G.; Li, C.; Shen, J. Y.; Chen, Z. J.; Shi, G. J. *Phys. Chem. C* **2007**, *111*, 5926. (b) Zhang, X.; Manohar, S. K. *J. Am. Chem. Soc.* **2005**, *127*, 14156.

(22) Huang, K.; Zhang, Y.; Long, Y.; Yuan, J.; Han, D.; Wang, Z.; Niu, L.; Chen, Z. *Chem.—Eur. J.* **2006**, *12*, 5314.

(23) S. Sarma, T. S.; Chowdhury, D.; Paul, A.; Chattopadhyay, A. *Chem. Commun.* **2002**, 1048.

Scheme 1. Procedure for the Synthesis of Various Anisotropic Au/PANI Nanostructures<sup>a</sup>

<sup>a</sup> The various products obtained are numbered.

PANI composite with gold particles of 0.8–1  $\mu\text{m}$  size range<sup>24a</sup> using  $\text{HBF}_4$  as the reducing agent has also been documented. We have shown that aniline can be polymerized in the presence of  $\text{Au}^{3+}$  forming PANI-coated spherical nanoparticles.<sup>24b</sup>

Our current investigations reveal the capping ability as well as the reduction capacity of aniline toward the synthesis of variety of interesting 1D and 2D anisotropic nanostructures of gold. In this paper, we present a simple low-temperature route for the synthesis of various water soluble PANI-based gold nanostructures starting from  $\text{Au}^{3+}$  and aniline. Interestingly, we observed the pH-dependent transformation of Au/PANI nanowires into various shapes. All the structures synthesized by the present method were highly stable. The effect of synthetic parameters on the morphology and size of the nanostructures was checked. These nanostructures were characterized using various spectroscopic and microscopic techniques, and a possible mechanism for the formation of nanowires is proposed.

### Experimental

**Materials.** Aniline was purchased from Sigma Aldrich and distilled twice under reduced pressure before use. Tetrachloroauric acid trihydrate ( $\text{HAuCl}_4 \cdot 3\text{H}_2\text{O}$ ) and citric acid were purchased from CDH, India. Polyvinylpyrrolidone (PVP) and potassium iodide were purchased from Merck. All chemicals were used as such without further purification. Triply distilled water was used throughout the experiments.

Scheme 1 shows the experimental procedure employed for making various nanostructures. We succeeded in making nanostructures such as nanowires, nanoplates, nanospheres, core–shells, needle-like aggregates, and flower-like particles. These products are numbered and these are used in the subsequent discussion.

The synthesis involves the following steps.

#### Synthesis of Oligoaniline-Coated Gold Nanoparticles (AuNPs).

In a typical synthesis, 25 mg of citric acid was dissolved in 35 mL of water. The solution was kept at 80  $^\circ\text{C}$  and 1 mL of 25 mM

$\text{HAuCl}_4$  was added. After 10 min, when the color changed from pale yellow to pink, 100  $\mu\text{L}$  distilled aniline was added followed by 500  $\mu\text{L}$  of 25 mM  $\text{HAuCl}_4$ . Heating was continued for 5 more minutes. The color of the solution changed to light pink, and a black precipitate was formed. This solution was kept at room temperature for 5 h, centrifuged at 4000 rpm, and the black residue was discarded. The resultant light pink supernatant, which contains oligoaniline capped gold nanoparticles, was used for further reaction.

**1. Synthesis of Au/PANI Gold Nanowires (1).** 2 mL of the as prepared oligoaniline-coated AuNPs were taken in a sample bottle. 2 mL of aqueous PVP (20 mg/mL) was added and the solution was kept in an ice bath. 500  $\mu\text{L}$  of 25 mM  $\text{HAuCl}_4$  was added in the cold condition. This solution was kept at 0  $^\circ\text{C}$  for 5 h. After 5 h, the color of the solution turned green. It was again centrifuged and further analyzed. This gave longer nanowires. For the synthesis of smaller Au/PANI nanowires, the above-mentioned procedure was repeated using the oligoaniline AuNPs synthesized using 10  $\mu\text{L}$  of aniline. This reaction happened even in the absence of PVP. But the stability of the resultant product at room temperature was less. Explanation is given in the text.

**2. Conversion of Au/PANI Nanowire (1) into Spherical Gold Nanoparticles (2).** In order to get spherical AuNPs, the pH of the longer Au/PANI nanowires synthesized in step 1 was changed to 10.2 by adding aqueous NaOH.

**3. Synthesis of Needle-like Aggregates (3).** As prepared longer Au/PANI nanowires (1) were maintained at a pH of 2.5 by adding HCl to get the needle-like aggregates.

**4. Synthesis of Core–Shell Nanoparticles (4).** The spherical nanoparticles prepared in step 2 were converted to core–shell geometry by the reversal of pH from 10.2 to 2.9 by the slow addition of HCl.

**5. Synthesis of Gold Nanoplates (5).** Oligoaniline AuNPs were synthesized by adding 250  $\mu\text{L}$  aniline and by repeating the procedure used for the synthesis of Au/PANI nanowires (1).

**6. Synthesis of PANI-Coated Flower-like Gold Nanoparticles (6).** The as prepared oligoaniline AuNPs (2 mL) were taken in a sample bottle. 2 mL of PVP solution (20 mg/mL) was added followed by 200  $\mu\text{L}$  of 2% KI. The solution was kept in an ice bath, and 500  $\mu\text{L}$  of ice cold 25 mM  $\text{HAuCl}_4$  was added to it. The resultant solution was kept at 0  $^\circ\text{C}$  for 5 h. The color of the solution turned to green

(24) (a) Kinyanjui, J. M.; Hatchett, D. W.; Smith, J. A.; Josowicz, M. *Chem. Mater.* **2004**, *16*, 3390. (b) Subramaniam, C.; Tom, R. T.; Pradeep, T. *J. Nanopart. Res.* **2005**, *7*, 209. (c) Liu, G.; Freund, M. S. *Macromolecules* **1997**, *30*, 5660.

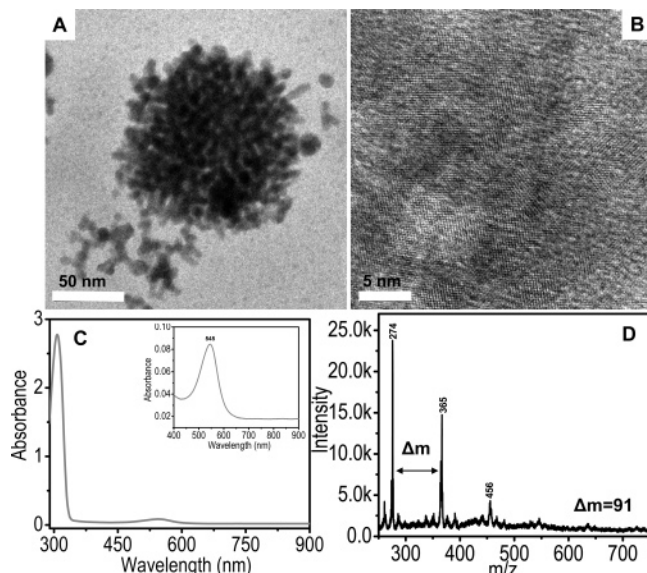


**Figure 1.** (A) TEM image of a single oligomeric-aniline-coated AuNP aggregate. (B) A lattice-resolved TEM image taken from the same nanoparticle. (C) UV-vis spectrum of oligomeric aniline-coated AuNPs. (D) LDI MS of oligoaniline-coated AuNPs. Inset of panel C shows an enlarged portion of the absorption spectrum.

along with the formation of sand-like particles. The solution was centrifuged, and the residue was analyzed.

**Instrumentation.** Transmission electron microscopy (TEM) was carried out using a JEOL 3011 300 kV instrument with a UHR polepiece. The samples for TEM were prepared by dropping the dispersion on amorphous carbon films supported on a copper grid and dried in ambience. Scanning electron microscopic (SEM) images were taken in a HITACHI S-4800 FE-SEM instrument. UV-visible spectra were measured using a Perkin-Elmer Lambda 25 spectrometer. For the infrared spectra, vacuum-dried samples were made in the form of KBr pellets, and the spectra were measured with a Perkin-Elmer Spectrum One FTIR spectrometer. Laser desorption/ionization mass spectrometric (LDI MS) studies were conducted using a Voyager DE PRO Biospectrometry Workstation (Applied Biosystems) matrix-assisted laser desorption/ionization time-of-flight mass spectrometer (MALDI-TOF MS). A pulsed nitrogen laser of 337 nm was used (maximum firing rate, 20 Hz; maximum pulse energy, 300  $\mu$ J) for the LDI MS studies. Mass spectra were collected in positive and negative modes and were averaged for 100 shots. X-ray diffraction (XRD) data were collected with a Shimadzu XD-D1 diffractometer using Cu K $\alpha$  radiation ( $\lambda = 1.54 \text{ \AA}$ ). The samples were scanned in the  $2\theta$  range of  $10\text{--}90^\circ$ .

## Results and Discussion

All the nanostructures were synthesized from oligoaniline-coated AuNP precursors. In order to get a stable oligoaniline nanoparticle, we have used a ligand exchange method. The nanoparticles formed were stable for a few months and were highly soluble in water. Figure 1A shows the TEM image of a single oligoaniline-coated Au nanoparticle. From the TEM image, it is confirmed that these are the raspberry-like aggregates<sup>25a</sup> of smaller nanoparticles of  $\sim 3 \text{ nm}$  diameter forming  $75\text{--}100 \text{ nm}$  structures. A lattice resolved image of an individual nanoparticle is given in Figure 1B. Optical absorption spectrum and TEM images of the oligoaniline AuNPs were comparable with those of Shiigi et al.,<sup>25a</sup> where they followed a different method of

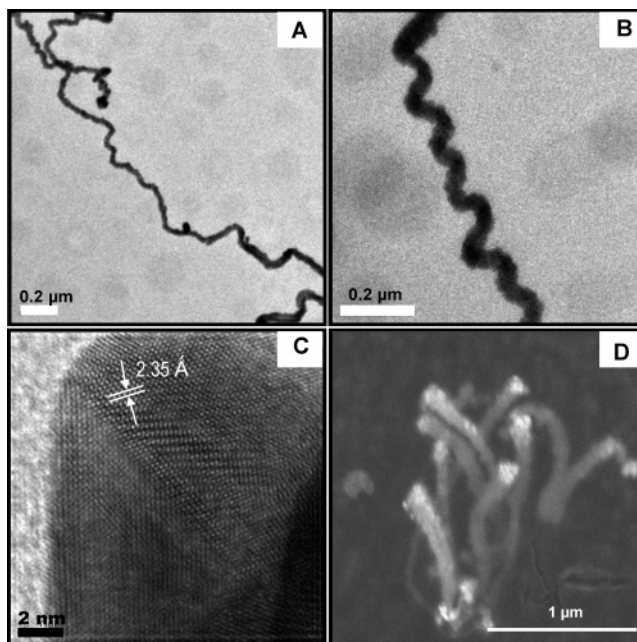


**Figure 2.** TEM images of gold nanowires at various magnifications when  $100 \mu\text{L}$  aniline was used. (C) The lattice resolved image of one part of the nanowire. (D) The SEM image of the gold nanowire synthesized in the same condition.

synthesis. Figure 1C shows the UV-vis spectrum of oligoaniline-coated Au nanoparticles. The peak observed at  $545 \text{ nm}$  (inset of panel C) is composed of features due to the excitonic-type transition in the quinoid unit of oxidized aniline and the surface plasmon of gold.<sup>25b,c</sup> The absorption at  $\sim 315 \text{ nm}$  is attributed to the  $\pi\text{--}\pi^*$  transition of phenylene rings. Supporting Information Figure S1 shows the TEM images of the oligoaniline AuNPs at various magnifications prepared using  $100 \mu\text{L}$  of aniline. The presence of oligoaniline is further confirmed by measuring the LDI MS of these nanoparticles. Figure 1D shows the LDI mass spectrum of oligoaniline-coated AuNPs between  $m/z$  250 and 750. The periodicity is characteristic of a polymer. The fragmentation peaks clearly indicates the presence of oligomers up to the 5-mer. These oligomers are separated from one another by a mass difference  $\Delta m = 91 \text{ Da}$ , which corresponds to the monomer ( $-\text{C}_6\text{H}_4\text{--NH-}$ ). It was noted that these nanoparticles, after drying on a clean cover glass, formed needlelike microstructures with needles projecting out from the surface. These microstructures were soluble in water and yield the same structures upon solvent evaporation. Panels A and B of Figure S2 (Supporting Information) show the SEM images of the needlelike microstructures formed on an indium tin oxide (ITO) conducting glass surface after drying the oligoaniline-coated AuNPs. Panels C and D of Figure S2 show the optical micrograms of these structures. Both SEM and optical micrograms show that these structures are several tens of micrometers in size. Formation of needlelike aggregates of metal nanoparticles incorporated in polyaniline and substituted polyaniline has been observed before.<sup>26</sup> Oxidation of aniline generates electrons which reduce the auric ions into Au atoms. Simultaneously, polymerization of aniline happens. These Au atoms subsequently coalesce and form clusters, which are stabilized within the growing polymer forming microstructures upon drying. The presence of citric acid (CA) in the solution makes an oligoaniline/CA salt form needlelike microstructures upon drying on glass substrates.<sup>27</sup> We made

(25) (a) Shiigi, H.; Yamamoto, Y.; Yoshi, N.; Nakaob, H.; Nagaoka, T. *Chem. Commun.* **2006**, 4288. (b) Liu, S.; Zhu, K.; Zhang, Y.; Zhu, Y.; Xu, J. *Mater. Lett.* **2005**, *59*, 3715. (c) Dufour, B.; Rannou, P.; Travers, J. P.; Pron, A.; Zagórska, M.; Korc, G.; Kulszewicz-Bajer, I.; Quillard, S.; Lefrant, S. *Macromolecules* **2002**, *35*, 6112.

(26) (a) Mallick, K.; Witcomb, M. J.; Dinsmore, A.; Scurrill, M. S. *J. Mater. Sci.* **2006**, *41*, 1733. (b) Mallick, K.; Witcomb, M. J.; Dinsmore, A.; Scurrill, M. S. *Langmuir* **2005**, *21*, 7964.

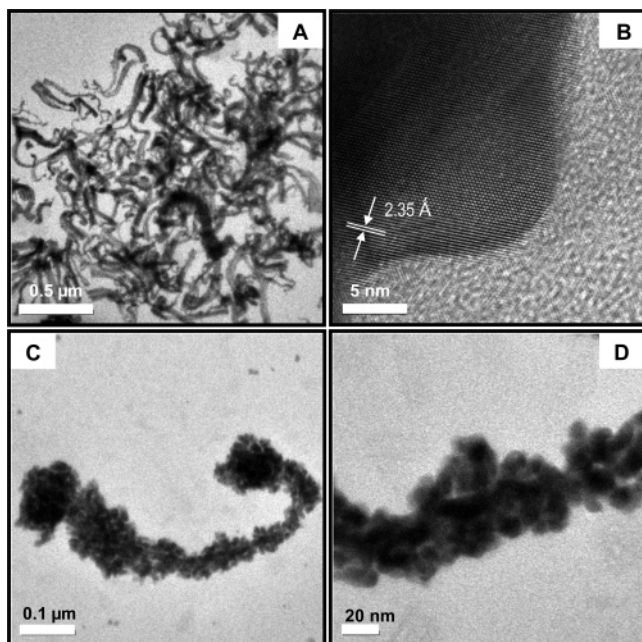


**Figure 3.** TEM images of gold nanowires at various magnifications formed when 10  $\mu\text{L}$  aniline was used. (B) The lattice resolved image of a part of the nanowire. (C) The TEM image of a single nanowire. (D) An enlarged portion of (C).

various anisotropic nanostructures from these nanoparticles. Interestingly, we found that the amount of aniline plays an important role in determining the size and shape of the resulting nanostructures.

Figure 2A is the representative TEM image of a single gold nanowire derived from oligoaniline-coated gold nanoparticles (1). Such wires were present in various parts of the grid. The image reveals that the wires exhibit a twisted structure. These nanowires have more than 2  $\mu\text{m}$  length and 60–70 nm diameter. Figure 2B shows the possible existence of the nanowires in a helical form. A magnified TEM image of the nanowire is shown in Figure 2C. The Au nanowires have a  $d$  spacing of 2.35  $\text{\AA}$ , which corresponds to the (111) crystal plane of gold (Figure 2C).

A typical SEM image of the gold nanowire synthesized in the same condition is given in Figure 2D. The SEM image shows that some of the gold nanowires are projecting out from the ITO conducting glass substrate. The poor clarity of the picture is due to the polyaniline coating and also due to the possible motion of the nanowire tips as they are supported only at the base. Panels A and B of Figure S3 (Supporting Information) show the large area SEM images of the longer nanowires formed. The XRD pattern of these nanowires (see Figure S4, Supporting Information) exhibits the reflections characteristic of gold, and

all the peaks can be indexed to face-centered cubic structure which confirms that the nanowires are composed of pure gold.

The synthesis was carried out with a precursor nanoparticle which was prepared at different concentrations of aniline. Figure 3A shows a large area TEM image of the nanowires formed when the reaction was carried out with the oligoaniline-coated gold nanoparticles synthesized using 10  $\mu\text{L}$  of aniline. A comparative reduction in the length of the nanowires is observed at this condition. Figure 3C represents the TEM image of a single nanowire. The length of the nanowires was around 1  $\mu\text{m}$ . From the TEM image (Figure 3D), it is clear that the surfaces of the nanowire were not as smooth as those of the longer nanowires synthesized in step 1. These nanowires are decorated with granular gold nanoparticles. As the wire is a three-dimensional structure, the entire structure is not focused properly at high magnifications and the image looks diffused. Figure 3B shows a lattice-resolved image of one portion of the nanowire. The lattice spacing of 2.35  $\text{\AA}$  observed in the nanowire corresponds to Au(111). The reduction in the size of the nanowire may be due to the smaller polyaniline chains formed during the synthesis at this low concentration of aniline. Throughout the synthesis, it was noted that low temperature favors the reaction. If the aniline concentration was increased to 250  $\mu\text{L}$  in step 1, the resultant product (at the end of step 5) was gold nanoplates (5). Figure 4 shows the SEM image of the nanoplates formed in step 5. From a magnified SEM image, it is clear that the nanoplates have  $\sim 1 \mu\text{m}$  length and thickness less than 100 nm. There was no nanowire formation at this condition. At higher concentration of aniline, the amount of oligoaniline formed will be comparatively high. So, under these conditions, the oligoaniline will adsorb prominently on the low index planes of the nanoparticles, which suppresses the overall crystal growth, resulting in the formation of nanoplates. Similar observations were reported by Bai et al.<sup>28</sup> during the synthesis of poly(acrylic acid) (PAA)-based silver nanobelts, which converted into nanoplates at higher concentrations of PAA.

This possibility is further confirmed by conducting the nanowire synthesis in presence of KI. It is reported<sup>29</sup> that the growth of nanoparticles can be tuned by the halide ions. We carried out the reaction, explained in step 6, in the presence of KI. Iodide can adsorb on certain planes of Au and can alter the growth of the nanoparticles. The lattice strain generated by the addition of the halide ions resulted in a morphology change of the nanoparticles. Interestingly, under this condition, flower-like nanostructures made of leaf-like subunits were formed (6). The monodispersity of the product was very high, and it was noted that the growth of nanowires was completely inhibited by the iodide ions. Panels A and B of Figure 5 show TEM and SEM images, respectively, of the nanostructures formed.

In order to study the course of the reaction, we monitored the UV–vis spectrum of the reaction mixture at various stages of

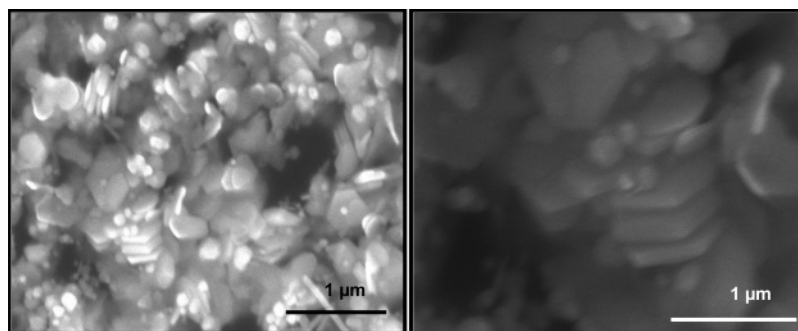


**Figure 4.** SEM images of the gold nanoplates formed when the reaction was carried out using the oligoaniline AuNPs synthesized by using 250  $\mu\text{L}$  of aniline.

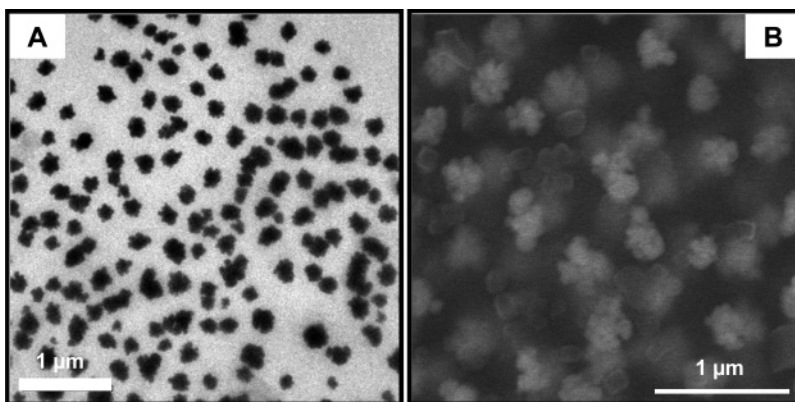


**Figure 5.** TEM (A) and SEM (B) images of the flower-like nanoparticles formed in the presence of KI.

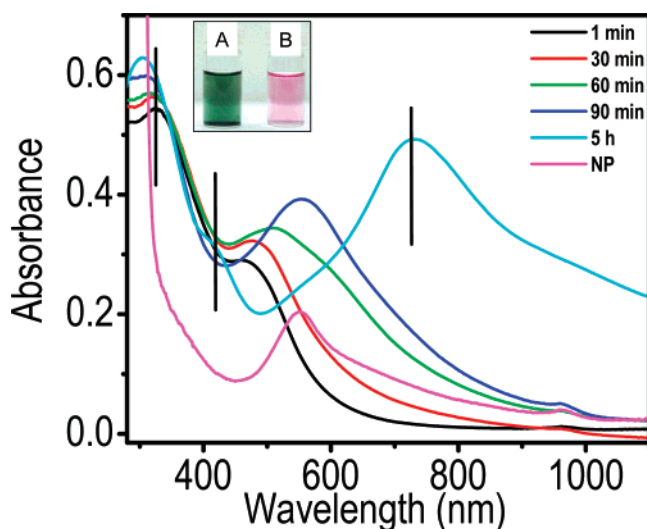


**Figure 6.** Time-dependent UV-vis spectra showing the formation of PANI-coated gold nanowires. The absorptions of PANI are marked. Inset shows the photographs of (A) the PANI-coated nanowire and (B) the precursor nanoparticle solution.

the reaction (Figure 6). After the immediate addition of  $\text{Au}^{3+}$  into the nanoparticle/PVP precursor mixture, the color of the solution changed drastically from pale pink to dark brown and a concomitant change was observed in the UV-vis spectrum. The absorption maximum of the solution changed from 545 to 475 nm. The absorption at 475 nm is attributed to the surface plasmon resonance of the smaller nanoparticle formed from the parent aggregate. As time proceeds, the absorption maximum at 475 nm showed a gradual red shift. After the completion of the reaction, the color of the solution changed to green and showed an absorption maximum at 730 nm (inset of Figure 6 shows the photographs of the nanowire solution and the precursor nanoparticle solution). Throughout the reaction, we have used PVP. It has been reported<sup>30a</sup> that PVP is effective for the dispersion polymerization of aniline. It can act as a steric stabilizer such that it can prevent the precipitation of polymerized aniline and make finely dispersed PANI in solution. By the addition of  $\text{HAuCl}_4$  into a solution containing PVP and oligoaniline/AuNPs, the  $\text{HAuCl}_4$  protonates free amino groups of oligoaniline and forms anilinium cations. Subsequently, this oligoaniline poly-

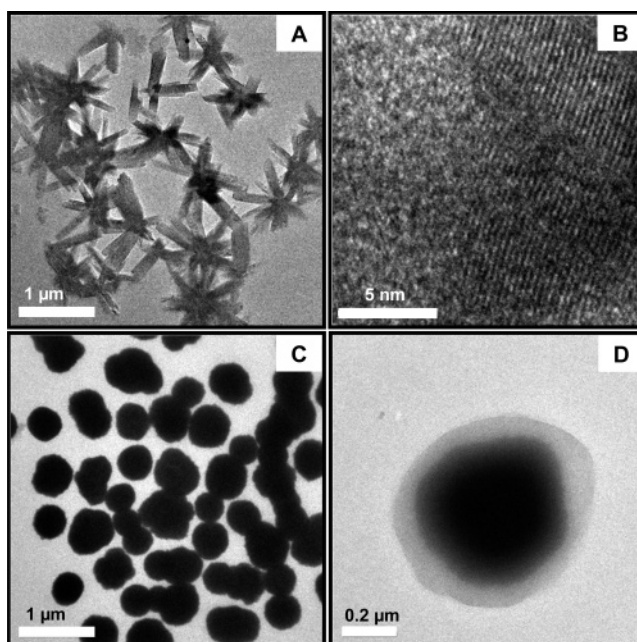


**Figure 7.** (A) TEM image of the nanowires at pH 2.5. (B) The lattice-resolved image of a region in A. (C) The TEM image of the nanowire at pH 10.2. (D) TEM image of the nanowire after the reversal of the pH from 10.2 to 2.9.

merizes. The free electron generated during the polymerization reduces  $[\text{AuCl}_4]^-$  to gold. Simultaneously the polymer chains self-assemble to form wirelike structures. The oligomeric intermediates adsorb on the stabilizer (PVP), and the PANI chains grow from these sites.<sup>30b</sup> This stabilizer prevents the aggregation of PANI. In presence of PVP, the nucleation of oligomers will be uniform. This polymerization and self-assembly of Au clusters will happen even in the absence of PVP. But in the absence of the stabilizer, the polyaniline aggregates in the reaction mixture and forms polydispersed macrostructures of Au/PANI. The nanowires formed in the absence of PVP had a rough surface, and the yield of the reaction was very less. The surface plasmon resonance of the nanowire is hidden by the intense absorption of PANI and appears as a shoulder in between 570–590 nm. The three absorption bands observed at 310, 425, and 730 nm (marked in Figure 6) are the characteristic absorption bands of PANI. The absorption at  $\sim 310$  nm is due to the  $\pi-\pi^*$  band of PANI, and the polaron band appears at 425 nm. The peak at 730 nm is attributed to the localized polaron band of polyaniline.<sup>13</sup>

Just after the addition of  $\text{Au}^{3+}$ , the plasmon excitation of the nanoparticles blue shifted indicating the reduction of the particle size. This is further confirmed from the TEM image. Figure S5

(27) Zhu, Y.; Li, J.; Wan, M.; Jiang, L.; Wei, Y. *Macromol. Rapid Commun.* **2007**, *28*, 1339.

(28) Bai, J.; Qin, Y.; Jiang, C.; Qi, L. *Chem. Mater.* **2007**, *19*, 3367.

(29) (a) Singh, S.; Pasricha, R.; Bhatta, U. M.; Satyam, P. V.; Sastry, M.; Prasad, B. L. V. *J. Mater. Chem.* **2007**, *17*, 1614. (b) Ha, T. H.; Koo, H. J.; Chung, B. H. *J. Phys. Chem. C* **2007**, *111*, 1123.

(30) (a) Sulimenco, T.; Stejskal, J.; Krivka, I.; Prokes, J. *Eur. Polym. J.* **2001**, *37*, 219. (b) Stejskal, J.; Sapurina, I. *J. Colloid Interface Sci.* **2004**, *274*, 489.

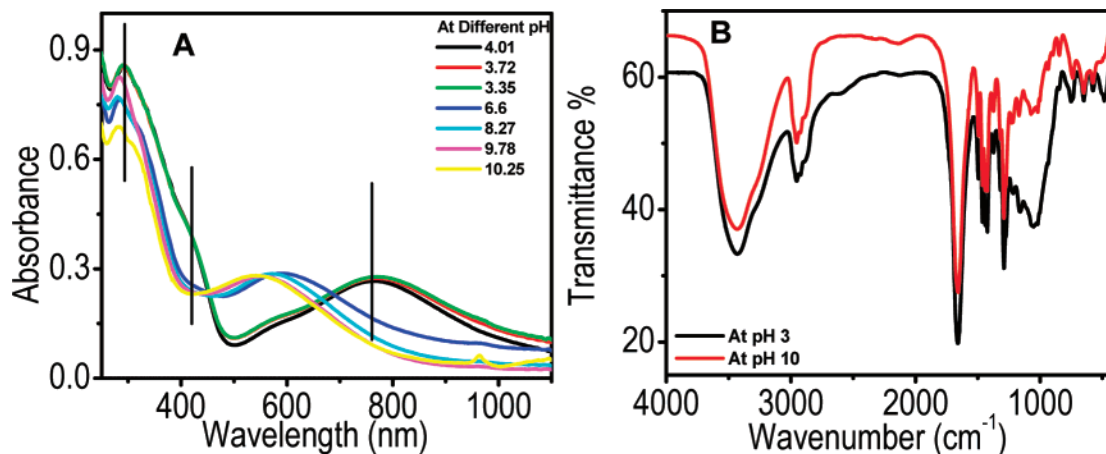


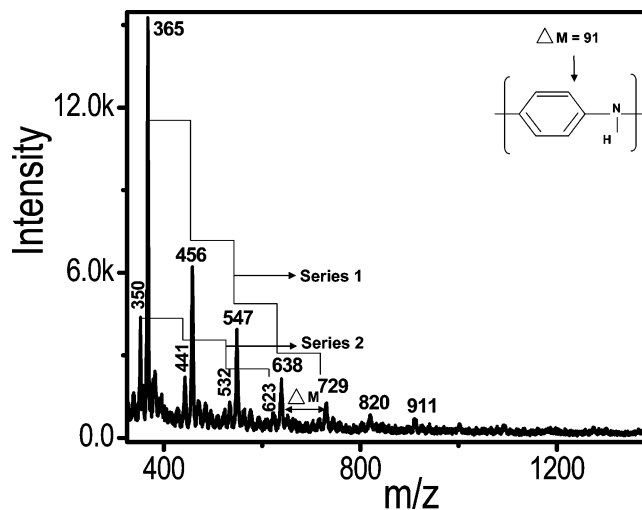
**Figure 8.** (A) The UV-vis spectra of the Au/PANI nanowire samples at different pH values, and (B) the IR spectra of the same sample at different pH values.

(Supporting Information) shows the TEM image of smaller nanoparticles formed after the immediate addition of the  $\text{Au}^{3+}$  into the solution containing PVP and oligoaniline AuNPs. TEM image reveals that these nanoparticles have a size of  $\sim 4$  nm. Subsequently, larger particles are formed, which show a plasmon excitation around 600 nm. Gradually, the PANI spectrum evolves, which masks the nanoparticle absorption. We have monitored the pH changes during the reaction. The pH of the PVP/nanoparticle solution decreased from 4.1 to 2.4 by the addition of  $\text{Au}^{3+}$ . After 10 min, the pH increased to 3 and reached to 3.7 toward the end of the reaction.

We have studied the change in morphology of the nanowire as a function of pH. When the pH of the nanowire solution made in step 1 was adjusted to acidic (pH 2.5) by adding HCl, the nanowires clustered into needlelike aggregates. Figure 7A shows the TEM image of the needle-like cluster formed at pH 2.5. The lattice resolved image (Figure 7B) shows that these needles are made of clusters of AuNPs. It was noted that the particles are not well dispersed and appear as clustered within the polymeric matrix. Under basic conditions (pH 10.2), the nanowires changed their morphology completely into spheres (2). Each of the particles had a diameter of 500–800 nm (Figure 7C).

As the pH changes, the color of Au nanowire/PANI solution changed from green (pH 2.5) to blue (pH 10.2). The color change is attributed to the existence of PANI in its emeraldine salt form and emeraldine base form. In order to check the reversibility of the morphology change of the nanowire, we changed the pH from 10.2 to 2.9 by adding HCl. Even though there was a change in the color from blue to green, the product obtained was entirely different. At this condition, we observed the formation of bigger core-shell like structures (4). Figure 7D reveals the core-shell geometry of the nanoparticles formed. During the reversal of pH, the PANI formed a shell around the gold nanoparticles. The size of these core-shell particles was 400–600 nm in diameter. The SEM images given in panels C and D of Figure S3 (Supporting Information) clearly show the formation of the core-shell nanoparticles. These observations indicate the strong influence of the pH on the shape transformations of the nanowires. The pH changes will destabilize the nanowires and rearrange it to yield more stable forms. We believe that the existence of different forms of PANI at different pH ranges may also trigger the formation of various templates.

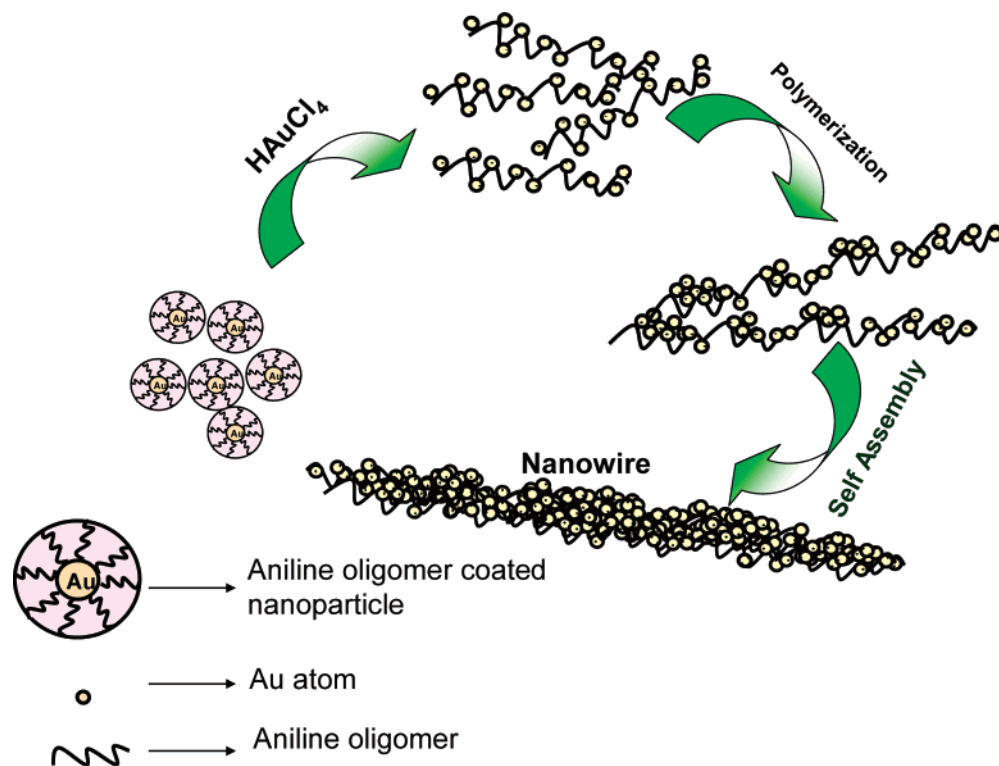
Figure 8A shows the pH-dependent UV-vis spectrum of the PANI-coated nanowire solution. The spectrum shows all the characteristic absorption due to PANI. This is consistent with the UV-vis spectrum of PANI prepared by the conventional



**Figure 9.** LDI mass spectrum of the PANI-coated gold nanowire taken in the linear positive mode.

method. Doping and de-doping of protons has been carried out by the addition of HCl and NaOH. By the addition of NaOH to the solution, Au/PANI composite changed into its basic form. The blue color of Au/PANI solution at basic pH is due to the existence of PANI in its emeraldine base form. After doping with HCl, the emeraldine base form of PANI is converted into emeraldine salt form with its characteristic three-absorption peak structure. We repeatedly doped and de-doped in order to check the stability of the product. By the addition of NaOH to the HCl-doped PANI-metal composite, the peak at 775 nm showed a gradual blue shift. When the pH of the solution was increased toward a basic value, the polaron band at 420 nm disappeared. A strong absorption band at 550–600 nm appeared, which is due to the exciton transition of the quinoid ring.<sup>31</sup> When the pH changed from 4 to 6.6, a sudden change was observed in the absorption maximum and the peak at 765 nm was shifted to 590 nm. This is attributed to the formation of the basic form of PANI. Because of the existence of PANI in different forms at acidic and basic pHs and because the pH range at which transition happens is narrow, the spectra show bunching both in the acidic medium (pH 3.35–4.01) and in the basic medium (pH 8.27–10.25). Even though we have not found any visual change after continuous

(31) (a) Epstein, A. J.; Ginder, J. M.; Zuo, F.; Bigelow, R. W.; Woo, H. S.; Tanner, D. B.; Richter, A. F.; Huang, W. S.; Macdiarmid, A. G. *Synth. Met.* **1987**, *18*, 303. (b) Zhu, C. L.; Chou, S. W.; He, S. F.; Liao, W. L.; Chen, C. C. *Nanotechnology* **2007**, *18*, 275604.

**Scheme 2. Illustration of the Proposed Mechanism for the Formation of PANI-Coated Gold Nanowire**


doping and de-doping, the morphology of the nanowire changed during this process, as explained earlier. The strong background in the PANI absorption after doping (Figure 8A) in the near-infrared region is due to polaronic absorption.<sup>32,33</sup>

FTIR spectrum of Au/PANI nanowire (Figure 8B) shows the characteristic peak of PANI at  $1501\text{ cm}^{-1}$ . This peak is mainly due to the C=C stretching of benzenoid ring of PANI. The peak at  $1300\text{ cm}^{-1}$  is due to the C-N stretching mode. As a result of intermolecular H-bonding,<sup>34</sup> the band for the carbonyl stretching frequency at  $1661\text{ cm}^{-1}$  of PVP<sup>35</sup> shifted to a lower value ( $1654\text{ cm}^{-1}$ ) in the PANI-PVP composite. The sharp peak around  $1435\text{ cm}^{-1}$  corresponds to the N-H deformation.<sup>35,36</sup> Even though both the IR spectra look similar, some of the peaks become broader and more intense after doping. This is attributed to the enhancement of the oscillator strengths of the PANI backbone related vibrations upon doping.<sup>37</sup> It is clear that the intensities of the peaks at  $1157\text{ cm}^{-1}$  and  $1034\text{ cm}^{-1}$  are increased after doping. The positive charge created on the polymer chain increases the molecular dipole moment which contributes to an increase in the vibrational intensity upon doping.<sup>38</sup>

The LDI mass spectrum of Au/PANI nanowire between  $m/z$  300 and 1400 is presented in Figure 9. Several peaks are observed, consisting of different polymer chains.<sup>39</sup> It is noticed that there are two series of peaks separated with  $m/z$  91, which indicates that the polymer motif is indeed aniline. The two series and the fragments observed are shown in Figure 9. These two series are

the result of the loss of terminal amine ( $-\text{NH}$ ) during the synthesis. The lower intensity peak is observed at a  $m/z$  15 lower than the main peak. It appears that the polymer chains are not long, or intact desorption does not occur as the PANI is bound to the metal surface at various points. The mechanism of the oxidation of aromatic amines in presence of  $\text{Au}^{3+}$  is discussed in our earlier paper.<sup>24b</sup> The electrons generated during the oxidation of aniline<sup>24c</sup> reduce the auric ions to Au atoms. Simultaneously, aniline polymerization and gold cluster formation happens. The strong affinity of gold toward nitrogen favors this process.

The possible growth mechanism responsible for the formation of nanowires is shown in Scheme 2. The immediate addition of  $\text{Au}^{3+}$  destabilizes the oligoaniline AuNPs system. The color change of the nanoparticle solution and corresponding blue shift in the UV-vis spectrum of the oligoaniline capped gold nanoparticle confirm the reduction of the particle size during the reaction. This has been confirmed by TEM measurements also. The unreacted aniline present in the system reduces  $\text{HAuCl}_4$ , leading to the formation of gold nanoclusters and aniline oligomers. Because of the increase in the size of the nanoparticles, the absorption maximum is red shifted. These nanoparticles will decorate on the oligoaniline present in the system. As time proceeds, the oligoaniline polymerizes to PANI. Finally, the AuNPs-decorated PANI will self-assemble<sup>22</sup> to form Au/PANI nanowires.

## Conclusion

We have demonstrated a simple and versatile method for the synthesis of PANI-based anisotropic gold nanostructures which include nanowires of various size, nanoplates, spherical and core-shell nanoparticles, flowerlike nanoparticles and needlelike aggregates. These structures were formed from precursor nanoparticles of gold stabilized by oligoaniline. We studied the pH-dependent shape transformation of the nanowire formed. Microscopic techniques such as TEM and SEM were used for the determination of the morphology of the nanostructures formed.

(32) (a) Zheng, W.; Min, Y.; MacDiarmid, A. G.; Angelopoulos, M.; Liao, Y. H.; Epstein, A. J. *Synth. Met.* **1997**, *84*, 63. (b) Schantz, S.; Torell, L. M.; Stevens, J. R. *J. Appl. Phys.* **1988**, *64*, 2038.

(33) Berzina, T.; Erokhin, V.; Fontana, M. P. *J. Appl. Phys.* **2007**, *101*, 24501.

(34) (a) Chen, S. A.; Lee, H. T. *Macromolecules* **1993**, *26*, 3254. (b) Armes, S. P.; Vincent, B. *J. Chem. Soc., Chem. Commun.* **1987**, 288.

(35) Ghosh, P.; Siddhanta, S. K.; Chakrabarti, A. *Eur. Polym. J.* **1999**, *35*, 699.

(36) Dispenza, C.; Presti, C. L.; Belfiore, C.; Spadaro, G.; Piazza, S. *Polymer* **2006**, *47*, 961.

(37) Wang, Y.; Rubner, M. F. *Synth. Met.* **1992**, *47*, 255.

(38) Ping, Z.; Nauer, G. E.; Neugebauer, H.; Theiner, J.; Neckel, A. *J. Chem. Soc., Faraday Trans.* **1997**, *93*, 121.

(39) Dolan, A. R.; Wood, T. D. *Synth. Met.* **2004**, *143*, 243.

FTIR, UV-vis, XRD, and LDI MS were used to characterize chemical composition of the nanostructures. Our method provides an effective way to design highly water soluble diverse 1D and 2D Au/PANI nanostructures with high colloidal stability. The polyaniline formed in situ can act as an effective template for making anisotropic nanostructures of various metals like palladium and platinum. These PANI-based anisotropic nanoparticles can act as active catalysts.<sup>19</sup> Metal incorporated conducting polymers will be useful for making conductive components in electronic devices. Therefore, such conducting polymer-coated 1D and 2D metal nanostructures could find applications in diverse areas.

**Acknowledgment.** We thank the Department of Science and Technology, Government of India for constantly supporting our research program on nanomaterials.

**Supporting Information Available:** TEM images of oligoaniline-coated AuNPs at various magnifications, SEM and optical micrograms of the oligoaniline/gold microstructures formed on ITO, SEM images of the Au/PANI gold nanowires and core-shells, XRD of Au/PANI nanowires, and TEM image of the intermediate nanoparticles formed after the addition of Au<sup>3+</sup> into nanoparticle/PVP solution. This material is available free of charge via the Internet at <http://pubs.acs.org>.

LA703593C